The Astrophysical Journal, 664:47–52, 2007 July 20

BIMODAL ACTIVE NUCLEI IN BIMODAL GALAXIES

A. Cavaliere[1] and N. Menci[2]
Received 2006 November 10; accepted 2007 April 16

ABSTRACT

By their star content, the galaxies split out into a red and a blue population; their color index peaked around $u-r \approx 2.5$ or $u-r \approx 1$, respectively, quantifies the ratio of the blue stars newly formed from cold galactic gas, to the redder ones left over by past generations. On the other hand, on accreting substantial gas amounts the central massive black holes energize active galactic nuclei (AGNs); here we investigate whether these show a similar, and possibly related, bimodal partition as for current accretion activity relative to the past. To this aim we use an updated semianalytic model; based on Monte Carlo simulations, this follows with a large statistics the galaxy assemblage, the star generations, and the black hole accretions in the cosmological framework over the redshift span from $z = 10$ to $z = 0$. We test our simulations for yielding in close detail the observed split of galaxies into a red, early and a blue, late population. We find that the black hole accretion activities likewise give rise to two source populations: early, bright quasars and later, dimmer AGNs. We predict for their Eddington parameter $\lambda_{\rm E}$—the ratio of the current to the past black hole accretions—a bimodal distribution; the two branches sit now under $\lambda_{\rm E} \approx 0.01$ (mainly contributed by low-luminosity AGNs) and around $\lambda_{\rm E} \approx 0.3$–1. These not only mark out the two populations of AGNs, but also will turn out to correlate strongly with the red or blue color of their host galaxies.

Subject headings: black hole physics — galaxies: evolution — galaxies: nuclei — quasars: general

1. INTRODUCTION

With the beginning of the 2000s the galaxies—long known to differ by articulated morphologies (see Sandage 2005)—have been recognized to neatly split by the colors of their stellar content into two populations of red or blue objects (Strateva et al. 2001; Baldry et al. 2004).

The *red* population comprises giant spheroidal galaxies larger than $M \approx 10^{12}\ M_\odot$. These are found to be in place by redshifts $z \approx 2$ when the universe was only a fifth of its present age; thence they evolved "passively" by declining stellar birthrates. So they appear as precociously "red and dead," marked by low values around 0.1 of the ratio $\eta = L_U/L_R$ of the UV-blue to the red luminosity, that is, by a color index $u-r = -2.5 \log \eta \approx 2.5$ (AB photometric system). The *blue* population, instead, is mainly comprised of smaller galaxies featuring a spheroidal bulge but also a conspicuous disk, with star formation still lively today so as to retain values $\eta \approx 1$ ($u-r \approx 1$).

These two populations correlate with their environment, with the former mainly inhabiting dense, crowded sites like groups or clusters of galaxies, and the latter widely distributed in the "field." The color bimodality is being traced (Bell et al. 2004; Giallongo et al. 2005) into the deep universe out to $z \approx 2$ when the galactic morphologies were mixed or clumpy (see Elmegreen et al. 2007).

The other component, harbored at the very center of most bright galaxies, is a massive black hole (BH; see Ferrarese & Ford 2005) with mass in the range $M_\bullet \approx 10^6$–$10^9\ M_\odot$. This is some 10^{-3} of the mass in the host spheroidal bulge; but on accreting a comparable mass at rates up to $\dot{M}_\bullet \approx 10^2\ M_\odot\ {\rm yr}^{-1}$ converted to energy at 10% efficiency, these BHs easily outshine all the galactic stars as active galactic nuclei (AGNs) or quasars radiating for some 10^8 yr bolometric luminosities up to $L \approx 0.1c^2\dot{M}_\bullet \approx 10^{14}\ L_\odot$. When this exceeds the Eddington luminosity $L_{\rm E} = 3 \times 10^4 M_\bullet\ L_\odot/M_\odot$ the very radiation pressure can blow away a surrounding source, whereas at $L = L_{\rm E}$ the mass $M_\bullet$ is minimized. So the bright, early quasars observed (Fan et al. 2004) to radiate about $L \sim 10^{14}\ L_\odot$ at $z \approx 6$ must conservatively involve supermassive BHs with $M \approx 10^9\ M_\odot$ activated at Eddington levels $L/L_{\rm E} \approx 1$. Less clear conditions prevail in later and fainter AGNs; these we discuss next, with a focus on predicting the Eddington ratios $\lambda_{\rm E} = L/L_{\rm E} \propto \dot{M}_\bullet/M_\bullet$ that the observations estimate with still significant selections and uncertainties.

2. SEMIANALYTIC MODELING

We calculate the distributions of BHs and host galaxies together using a single semianalytic model (SAM); this links several astrophysical processes to yield the astronomical observables with a large statistics within manageable computer times.

The building blocks are provided by Monte Carlo simulations for the growth of the dark matter condensations (DM "halos") that dominate the mass in all cosmic structures from galaxies to their groups and clusters. As the universe ages, expands, and thins down, the primordial density fluctuations condense out on progressively larger scales by gravitational instability (cf. Peebles 1993). Their growth actually involves major mergers with comparable halos and coalescence with smaller ones; after each round a halo goes to a virial equilibrium with internal densities $\rho \approx 10^2 \rho_u(z)$ relative to its surroundings. Details of our computations are given in the Appendix. The building up of a large present-day galaxy through the above dynamical "merging histories" is illustrated in Figure 1.

As the DM halos are included into larger ones they may survive as subhalos holding galaxies; these, however, may coalesce at the center to form a dominant galaxy, or orbit for a while within the halo as satellite galaxies. In our simulations we compute in detail the dynamical processes causing evolution of these galaxies, namely: (1) the dynamical friction causing inspiral and leading to coalescence with the central galaxy; (2) the binary aggregations between two satellite galaxies orbiting within a common DM halo; and (3) other grazing encounters of galaxies not leading to merging, but affecting star formation and BH accretion (see below).

[1] Dipartimento Fisica, University di Roma "Tor Vergata," 00133 Rome, Italy.
[2] INAF–Osservatorio Astronomico di Roma, 00040 Monteporzio, Italy.

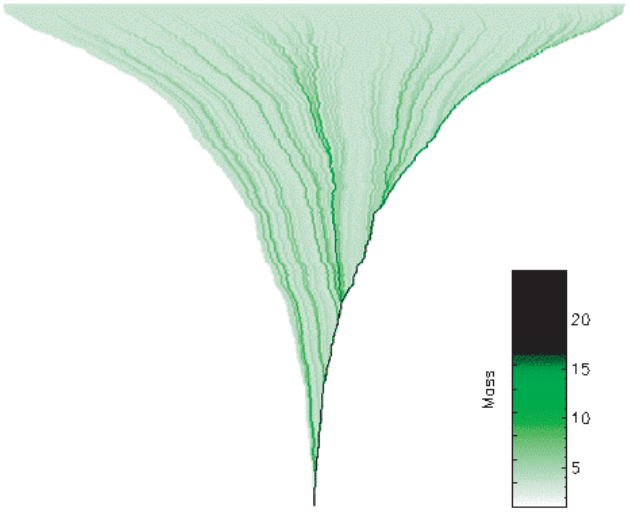

FIG. 1.—Merging tree from our Monte Carlo simulation, showing the formation history of a central dominant galaxy in a large DM halo with present mass $10^{13}\ M_\odot$. Time runs from top to bottom, from $z = 10$ to the present. Each branch represents a progenitor of the final galaxy, and the color code (shown on the right in units of $5 \times 10^{11}\ M_\odot$) quantifies the mass of the corresponding progenitor. A total of some 10^3 progenitors are involved, with the main one being represented on the rightmost branch.

As for the baryonic component, the dark halos provide gravitational wells for the visible galaxies to sit in and cycle baryons at densities large enough to form stars and grow BHs, as computed by SAMs (see the Appendix). Briefly, stars form quiescently at rates 1–10 $M_\odot\ \mathrm{yr}^{-1}$ after the classic Schmidt birthrate $\tau_*^{-1} \propto m_c/t_d$ in terms of the dynamical timescale t_d and of the mass m_c of cold galactic gas. The latter is modulated to a sensitive function of time $m_c(t)$ by a number of standard processes: consumption by the very star formation, depletion due to outflows caused by the energy fed back from supernova explosions ending the life of massive stars, and additions from initially virialized but radiatively cooled gas.

In addition, our SAM also includes impulsive star formation up to several $10^2\ M_\odot\ \mathrm{yr}^{-1}$, as occur in a protogalaxy when a collision with a companion stimulates a burst rich in blue-UV stars. From major mergers to minor merging to close flybys, these gravitational interactions distort the gravitational field and cause some galactic gas to lose angular momentum; thus, inflow and convergence are stimulated, and stars form in plenty at effective birthrates (see the Appendix; "Collisions and interactions") $\tau^{-1} = N\,\Sigma\,V \propto \rho(z) M^{2/3}$, a scaling that favors large galaxies at high z. A related feature of our SAM is the gas fraction from the same inflow that reaches farther down to the very center to fuel a massive BH and kindle quasar emissions (Cavaliere & Vittorini 2000, 2002; Menci et al. 2003; Hopkins et al. 2006). These in

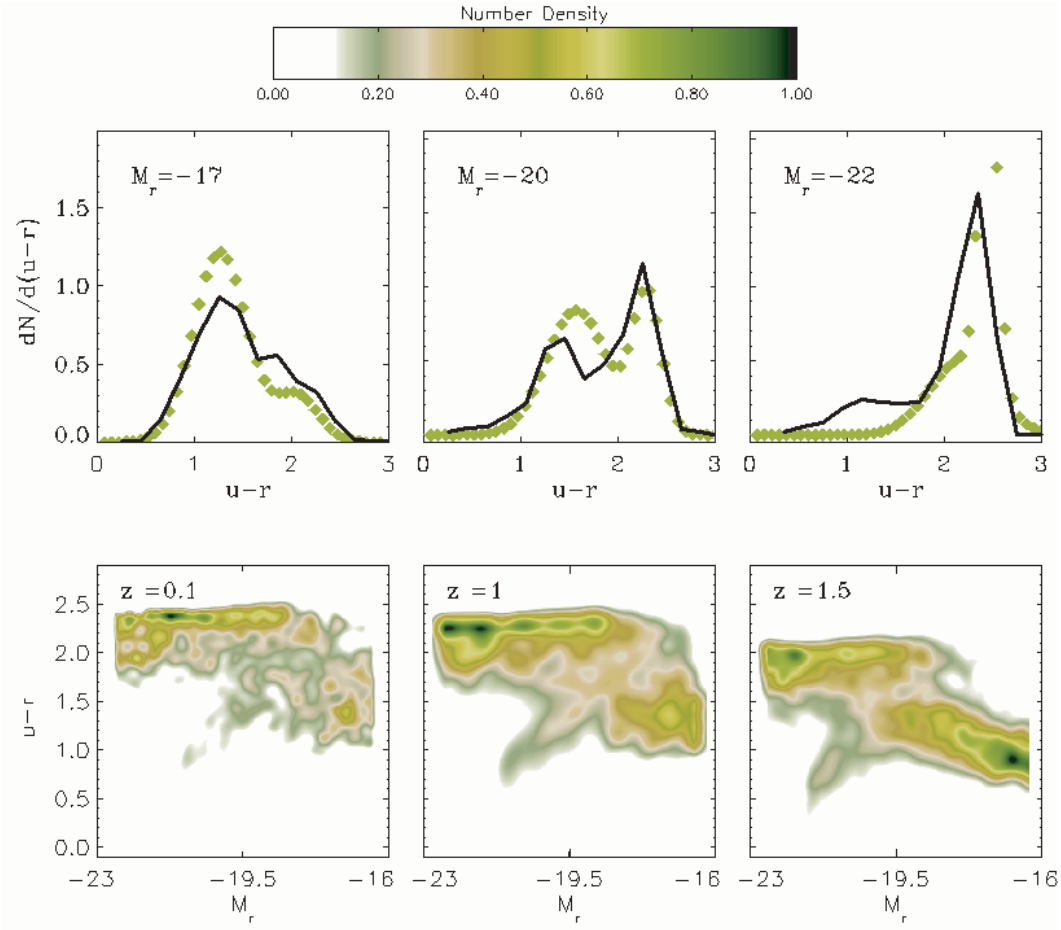

FIG. 2.—Bimodal galaxies from our SAM. *Top*: Plots of the present ($z = 0$) color distribution in the form of number density $dN/d(u-r)$ normalized to its maximum vs. the color index $u-r$, at different absolute magnitudes M_r in the red band. Clear bimodality appears as the bright population marked by red colors $u-r \approx 2.5$ ($\eta \approx 0.1$) peaks away from the fainter, bluer one ($u-r \approx 1$, $\eta \approx 0.4$), and compares well with the extensive observational statistics (*diamonds*; see Baldry et al. 2004). *Bottom*: Contour representation of the evolving color-magnitude relation that we predict at higher z. Bimodality persists out to $z = 1.5$, with the "red sequence" still separated by a "valley" from the "blue cloud"; while the latter is progressively stretched out into a richer "blue sequence," the former is progressively skewed toward the bright massive end.

turn cause violent energy feedback on the surrounding gas, to the point of halting accretion or even quenching all star formation; see also Di Matteo et al. (2005).

Linking and bringing to focus all these processes, our SAM yields galactic scaling laws and luminosity functions in agreement with the data at low and high z (see Menci et al. 2003, 2005). Next we highlight additional results and their interpretation.

3. BIMODAL GALAXIES

In Figure 2 we show our galaxy color distribution at $z \approx 0$, which splits out into a neatly *bimodal* population in detailed agreement with the observations; the lower panels articulate our projections to, and predictions at, higher z.

Clearly we are confronted with two effectively *different* chains of events started by the DM merging histories and amplified by the star formation processes, which we reconstruct as follows.

The growth of a halo is speeded up when its initial seed is biased high, i.e., grows in an *overdense* and *crowded* region of the primordial Gaussian fluctuations (Bardeen et al. 1986). The associated protogalaxies undergo more frequent mergers and other gravitational interactions (Conselice 2006) in the early, denser universe; thus, they build and light up precociously, and assemble into the large spheroidal galaxies with $M > 10^{12}\ M_{\odot}$ of today. Mergers occurring at protogalactic scales also replenish the gas masses m_c toward the cosmic ratio of baryons/DM ≈ 0.17; so the stellar birthrates are sustained up to several $10^2\ M_{\odot}\ \mathrm{yr}^{-1}$ in stimulated bursts.

But when (by $z < 2$) major galaxy merging becomes increasingly rare, the gas reservoirs rapidly run out and all stellar birthrates run down. Then the early era of efficient star formation comes to an end, leaving behind a multitude of reddish, sluggish stars that taint these large protogalaxies already early on while they assemble into the giant, red and dead galaxies of today.

Meanwhile, smaller galaxies assemble from lower mass progenitors growing up in the more common, *lower density*, and *quieter* regions of the primordial fluctuation field, and quiescently process their gas into stars at a lower but more even pace. So this other branch of histories leads to galaxies that retain larger amounts of cold gas, conducive to enduring if peaceful stellar birthrates and regeneration of massive stars with blue color.

In the long run, even these galaxies make a transition to the fully inefficient star-forming regime and turn red. This occurs after they undergo a late major merger (Conselice 2006) that triggers a gas-consuming star burst, or when they grow to a size such that gas cooling is inefficient (Dekel & Birnboim 2006), or eventually by sheer exhaustion of their cold gas reservoir. Overall, at cosmic ages later than $z \approx 2$ the actual star formation activity appears as if "downsized" toward smaller galaxies (Cowie et al. 1996).

Such specific evolutionary behaviors begin to be captured by recent models of galaxy formation (Menci et al. 2005; Bower et al. 2006; Cattaneo et al. 2006; Croton et al. 2006) and are focused by the present one in connection with the AGN behavior.

4. BIMODAL AGNs

Here we stress a related bimodality in radiative AGN activity, which we expect, since the galactic gas feeds both the star formation and the central BH accretion. Our SAM specifically links the bolometric AGN luminosity $L \propto fm_c$ to the cold gas amount $m_c(t)$ left over at the time t and to its fraction f stimulated to accrete; this is statistically distributed, since the interaction parameters are set by the merging history specific to each host galaxy. The (possibly repeated) accretion events accrue the summed mass $M_\bullet = \int dtL(t)/0.1c^2$ in the BHs that constitute the endpoints of gravitational collapse.

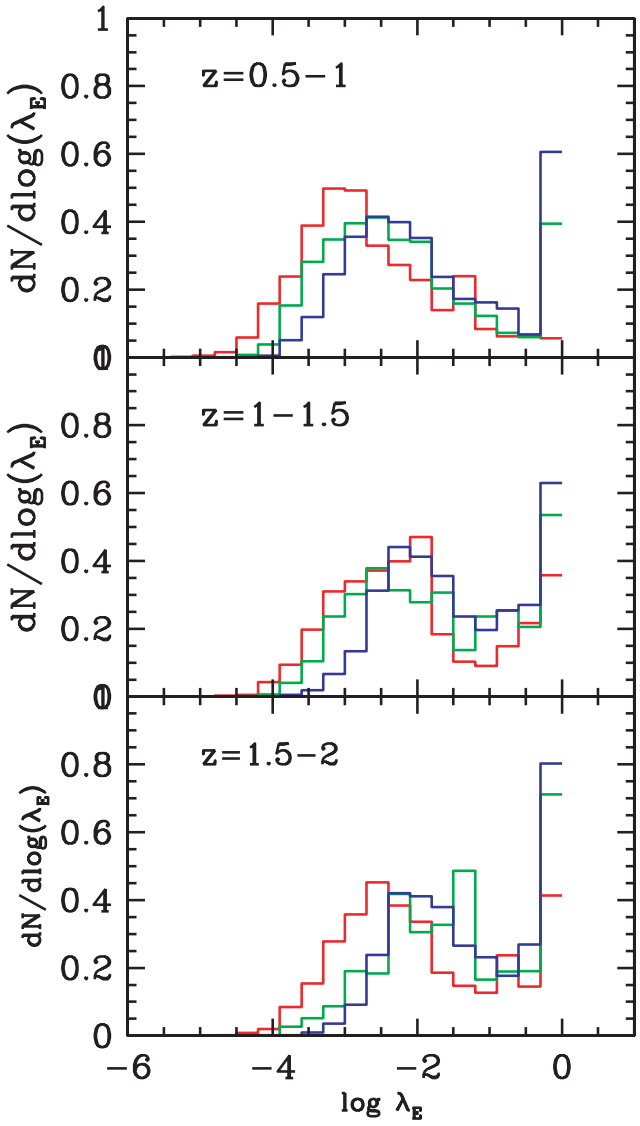

FIG. 3.—Bimodal AGNs from our SAM. In three redshift bins we show the distributions of λ_E for AGNs with different luminosities: $L > 10^{45}$ (*blue histogram*), $10^{44.5} \leq L \leq 10^{45}$ (*green histogram*), and $L < 10^{44.5}$ (*red histogram*); the distributions are normalized to the total content of each luminosity range.

From L and $M_\bullet$ we derive our predictions concerning the distributions of the Eddington parameters $\lambda_E = L/L_E$ and show them in Figures 3 and 4; we find the AGNs to exhibit a *bimodal* distribution of $\lambda_E \propto \dot{M}_\bullet/M_\bullet$ that quantifies the current relative to the past BH accretion. The content of the two branches changes with redshift; specifically, in the era of intense star formation for $z > 1.5$ most AGNs stay up to $\lambda_E \approx 0.3$–1, as observed (see McLure & Dunlop 2004; Vestergaard 2004), with the brighter AGNs skewed toward larger values of λ_E. At lower z, instead, we predict the branch with $\lambda \sim 10^{-2}$ to become increasingly richer mainly in low-luminosity ($L \lesssim 10^{44}$ ergs s^{-1}) AGNs, in accord with observations by Panessa et al. (2006) and findings by Lapi et al. (2006). We specifically predict (see Fig. 4) that at low redshifts most AGNs with very small λ_E are hosted in *red* galaxies, while those with larger values around $\lambda_E \approx 0.3$–1 are mainly hosted by *blue* galaxies.

This is because protogalaxies on the early, hectic branch of the merging histories process much of their gas content both into

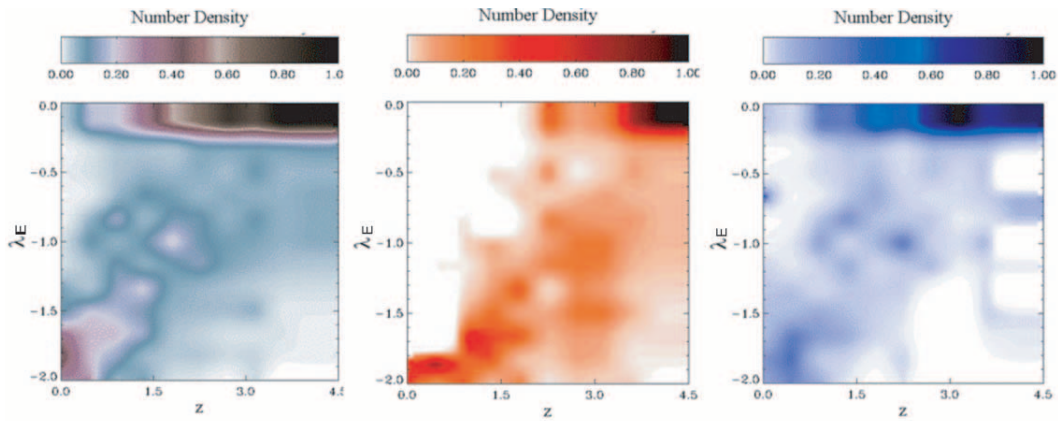

FIG. 4.—Bimodal AGNs from our SAM. *Left*: Overall evolution with z of the Eddington ratios λ_E for AGNs brighter than $L = 10^9\ L_\odot$; the code represents the number density of galaxies, normalized to the maximum value at each z. *Center*: Same, for the AGNs hosted in red galaxies ($u-r > 1.5$). *Right*: Same, for AGNs in blue galaxies ($u-r \leq 1$).

vigorous star formation, and into bright quasar activity sustained at full levels $\lambda_E \approx 1$ by frequent mergers and plenty of gas. But soon after $z \approx 2.5$ these activities concur to deplete the gas, and drive themselves into a steep decline. What remains of those flaming days—along with the multitude of red stars that taint such galaxies—are dozing or dormant supermassive BHs with trickling, inefficient accretion. So we expect the early quasar population that shone up at high z in dense environments to fall down in luminosity while retaining their large accrued BH masses; these features concur to confine the Eddington ratios to small values $\lambda_E \lesssim 10^{-2}$ in red hosts at low z.

Along the other, easygoing branch, smaller and gas-rich galaxies not only feed quiescent but persisting star formation and regenerate blue stars, but can also provide to smaller BHs material for sizeable accretion energizing a late AGN population (cf. observations by Kauffmann et al. 2003; Vanden Berk et al. 2006), when effectively stimulated. A main trigger is again provided by galaxy interactions, rare but persisting in the field; these cause gas inflows in the host, either directly or accruing to yield secular disk instabilities (see Combes 2005). The basic rate $\tau^{-1} \propto \rho$ (Cavaliere & Vittorini 2000; our Appendix) takes on values $\tau^{-1} \approx 0.1\ \mathrm{Gyr}^{-1}$ in the large-scale structures that streak the field with galaxy density contrasts $\rho/\rho_u \approx 3$–5, as compared to $\tau^{-1} \gtrsim 1\ \mathrm{Gyr}^{-1}$ in early small groups some 10 times denser.

These field interactions act on a gas content generally rich but variable in detail. Thus, we expect for the late AGN population values of λ_E considerably *exceeding* those in the red hosts at equal luminosities, but *scattered* in a wide distribution that can be accurately predicted only by a numerical code such as our SAM (see Figs. 3 and 4). On similar grounds one expects a wide scatter also for the values of η in the blue galaxy population, as in fact we had found and shown in Figure 2.

5. CONCLUSIONS AND DISCUSSION

In sum, physical evaluations borne out by our advanced SAM yield the articulated demographics illustrated by Figures 2, 3, and 4, and lead us to the following picture. The evolutions of the star glow and of the quasar-AGN shine may be collectively described as "downsizing" of all activities, but these are specifically marked by *bimodal* and *corresponding* ratios of current/past star generations ($\eta = L_U/L_R$) and current/past BH accretions ($\lambda_E \propto L/M_\bullet$). In fact, all baryon emissions are driven along two different evolutionary tracks by the DM merging histories (see Fig. 1); the difference is switched on as the tracks start from biased or from average regions in the fluctuation field, and is amplified by the baryonic histories.

Galaxies on biased tracks soon grow large, while interacting at brisk rates $\tau^{-1} \propto \rho(z)M^{2/3}$ that stimulate *frantic* bursts of star formation and BH accretion. Both activities live fast and die young by $z \approx 2$, when major mergers run down and galactic gas runs out; what remains of those flaming days are large masses stocked in red stars and in supermassive BHs. Along the average tracks, instead, all activities proceed at an *easier* pace that makes up lesser galaxies and BHs, but conserves gas for later use. These residual cold gas masses $m_c(t)$ can feed *persisting* star birthrates $\tau^{-1} \propto m_c$ that renew blue stars and bluish overall colors (see Fig. 2).

Meanwhile, the early and the late quasar-AGN populations differ even more. This is because red, gas-poor hosts can only feed fully grown BHs to yield feeble luminosities $L \propto m_c(t)$, on ineffective interactions in rich groups and clusters. Blue gas-rich hosts, instead, can supply to still underdeveloped BHs sizeable gas lumps to kindle them up, when stimulated by external events of *interaction* at rates $\tau^{-1} \propto \rho(z)$ slowly dwindling in the field.

In spite of the scatter imparted to the later AGN population by the increasingly sporadic fueling of their BHs, such a difference can be recognized (see Fig. 4) in the distribution of λ_E when this will be statistically correlated with host color $u-r$.

We thank our referee for comments useful toward tuning up our presentation.

APPENDIX

Framework.—We adopt the flat concordance cosmology (see Spergel et al. 2007) with Hubble expansion constant $H_0 = 70\ \mathrm{km\ s^{-1}\ Mpc^{-1}}$; the matter density with parameter $\Omega_0 = 0.3$ is dominated by the DM with a baryonic fraction 0.17.

Within this framework, the galaxy evolution is widely described by semianalytic modeling (SAM; e.g., Somerville et al. 2001; Bower et al. 2006). Our SAM includes, along with the standard processes, a number of novel features; key points follow, with details given in Menci et al. (2003, 2005).

Dynamical histories.—Our computations are started at $z = 10$ and cover the range of cosmic times down to $z = 0$ in 300 evenly spaced time steps. We take from Lacey & Cole (1993) the probability for a halo mass M condensed at a given time t to be merged into a larger mass $M + \Delta M$ at the time $t + \Delta t$, consistent with the classic Press & Schechter overall mass distribution. We run 5000 merging histories yielding at $z = 0$ a grid of 50 final halo masses with evenly spaced logarithmic values in the range 10^9–10^{15} $M_\odot$; for each we compute 100 realizations of merging histories.

The galaxy histories, started out by assigning a galaxy to each halo, soon take on a course of their own. As t proceeds and two halos merge, the embedded satellite galaxies may either coalesce with the dominant one by fast orbital decay due to dynamical friction, or engage in a binary "collision" with another satellite. When starting in a biased region, a history is speeded up; it is easily checked that galaxy size fluctuations growing in a group-sized one halve their collapse and quarter their interaction times.

Gas cooling.—Stars and BHs feed on cool gas. Initially the gas content of a halo is $m_c = 0.17M$, with a temperature at the virial value. The fraction that cools radiatively by line and continuous emissions is computed with standard procedures described in detail in Somerville & Primack (1999), Somerville et al. (2001), and Menci et al. (2005); the cooled gas is assigned to a disk (in keeping with the observations by Genzel et al. [2006] and Elmegreen et al. [2007]) in the dominant galaxy; radius $r_d \approx 2$ kpc and rotation velocity $v_d \approx 100$ km s^{-1} are computed after Mo et al. (1998), and specify the dynamical timescale to $t_d = r_d/v_d \approx 10^8$ yr. The disk is destroyed, and the stars are assigned to a bulge when a merging event involves a partner more massive than 1/3 of the main progenitor galaxy (major merger). A disk surrounding the bulge may form again when new gas in the halo is able to cool anew; this standard procedure is described in detail in Cole et al. (2000).

Quiescent star formation.—From the cooled gas stars form at the Schmidt rate $dm_*/dt = 0.1m_c/t_d$, to yield 1–10 $M_\odot$ yr^{-1}.

Supernova feedback.—Stars exceeding 8 $M_\odot$ end up in a supernova (SN) explosion that releases an energy $E_{\rm SN} = 10^{51}$ ergs. This reheats to the hot phase a gas mass $m_h = 3 \times 10^{-4} E_{\rm SN} m_*/v_c^2$ in halos with circular velocity v_c. In intermediate-small galaxies with $v_d < 120$ km s^{-1} (see also Dekel & Silk 1986; Dekel & Birnboim 2006) much cold gas is heated up or even pushed out, so as to enforce self-regulating star formation in a push-pull regime.

In addition to the above standard processes our SAM includes the following ones.

Collisions and interactions.—Our SAM includes merging and coalescence of galaxies within common DM halos, due to both orbital decay from dynamical friction, and random collisions with other satellite galaxies; the interplay between the two processes is discussed and illustrated in Menci et al. (2002). The timescale for dynamical friction and binary merging, and so the probability for such processes to occur in each time step, are given by equations (2) and (4) in Menci et al. (2002). We also compute the probability for a galaxy to undergo a grazing interaction with another satellite galaxy in a common DM halo. In each halo we compute the rate $\tau^{-1} = N \Sigma V$ of galaxy interactions from the current number density $N = \rho/M$ of galaxies with average relative velocity V and cross section Σ. This is close to the geometric value, to imply the scaling $\tau^{-1} \propto \rho M^{2/3}$, for the velocities $V \lesssim 2v_c$ as occur in small groups or in the field; on the other hand, Σ is quite smaller at the higher V occurring in rich groups or clusters.

Stimulated gas inflow.—Grazing interactions trigger starbursts and BH accretion (for relevant recent observations, see Borne et al. 2000; Komossa et al. 2003; Guainazzi et al. 2005). In fact, they destabilize the cold gas in the galactic disk from its rotational equilibrium so that a fraction of it inflows toward the center (see, e.g., Cox et al. 2006). Such a fraction is given by the perturbation $\Delta j/j$ of the gas specific angular momentum $j \approx GM/v_d$ induced by an interaction, in the form

$$f_{\rm acc} \approx \frac{1}{2} \left| \frac{\Delta j}{j} \right| = \frac{1}{2} \left\langle \frac{M'}{M} \frac{r_d}{b} \frac{v_d}{V} \right\rangle \tag{A1}$$

(Cavaliere & Vittorini 2000). Here b is the impact parameter, evaluated as the average distance of the galaxies in the halo; M' is the mass of the partner galaxy in the interaction, and the average runs over the probability of finding such a galaxy in the same halo where the galaxy M is located. All such quantities are computed in our Monte Carlo SAM. We calibrate the subfractions that go into starbursts (f_*) or into BH accretions ($f_\bullet$) after the limits set by IR and X-ray surveys of galaxies with stars or AGN energy sources (see Alexander et al. 2005; Franceschini et al. 2005). We define "stimulated" inflow as the quantity $f_{\rm acc} m_c/\Delta t = (f_* + f_\bullet) m_c/\Delta t$ destabilized in the time step Δt; this is converted into starbursts and BH accretion as described below. The relevance of such stimulated inflows has been extensively discussed and tested by our group and others (see Menci et al. 2003; Cox et al. 2004; Di Matteo et al. 2005; Vittorini et al. 2005).

Starbursts.—The stimulated inflow converging toward the nucleus forms starbursts at some 10^2 $M_\odot$ yr^{-1} for about 10^8 yr (see also Somerville et al. 2001), contributing a stellar mass $\Delta m_* = f_* m_c$, with average value $\langle f_* \rangle \approx 15\%$. The integrated mass so produced is smaller than from quiescent formation, but it prevails in large protogalaxies at $z > 2$.

Growth of massive BHs.—Initially, a seed BH with $M_\bullet \approx 100$ $M_\odot$ is assigned to each galaxy. At later t, this develops mainly by stimulated gas accretion, with average $\langle f_\bullet \rangle \approx 2\%$. The result is an accretion event of a mass $f_\bullet m_c \approx 10^{-3} M$ over a time close to t_d, recurring on a timescale τ.

AGN feedback.—The cold gas is reheated also by large and impulsive energy discharges from AGN activity, amounting to $\Delta E \approx 10^{62} M_\bullet/10^9$ $M_\odot$ ergs. On coupling with the surrounding gas at levels $\lesssim 5\%$ (bounded by momentum conservation between photons and gas particles) these injections match the binding energy even in large galaxies; thus, cold gas is reheated or expelled by superwinds and shocks (see Lapi et al. 2005).

Other AGN features.—Our SAM also yields the relation $M_\bullet/M_{\rm bulge} \approx 2 \times 10^{-3}$ recalled in the text, and quasar-AGN luminosity functions evolving in a bimodal fashion (Menci et al. 2003; see data by Hasinger et al. 2005): the bright early quasars peak sharply at $z \approx 2.5$ and drop by factors of some 10^{-3} by the present time; the numerous weaker AGNs selected in X-rays roll over a wide maximum around $z \approx 0.8$, with a weaker decline $z \approx 0$ by a factor of 10^{-1}. From the same SAM yielding these specific AGN features we recover the bimodal galactic colors $u-r$ shown in Figure 2, and predict the overall Eddington ratios $\lambda_{\rm E}$ in Figures 3 and 4.

REFERENCES

Alexander, D. M., Bauer, F. E., Chapman, S. C., Smail, I., Blain, A. W., Brandt, W. N., & Ivison, R. J. 2005, ApJ, 632, 736
Baldry, I. K., Glazebrook, K., Brinkmann, J., Zeljko, I., Lupton, R. H., Nichol, R. C., & Szalay, A. S. 2004, ApJ, 600, 681
Bardeen, J. M., Bond, J. R., Kaiser, N., & Szalay, A. S. 1986, ApJ, 304, 15
Bell, E. F., et al. 2004, ApJ, 608, 752
Borne, K. D., Bushouse, H., Lucaas, R. A., & Colina, L. 2000, ApJ, 529, L77
Bower, R. G., et al. 2006, MNRAS, 370, 645
Cattaneo, A., Dekel, A., Devriendt, J., Guiderdoni, B., & Blaizot, J. 2006, MNRAS, 370, 1651
Cavaliere, A., & Vittorini, V. 2000, ApJ, 543, 599
———. 2002, ApJ, 570, 114
Cole, S., Lacey, C. G., Baugh, C. M., & Frenk, C. S. 2000, MNRAS, 319, 168
Combes, F. 2005, in AIP Conf. Proc. 783, The Evolution of Starbursts: The 331st Wilhelm and Else Heraeus Seminar, ed. S. Huettemeister et al. (Melville: AIP), 43
Conselice, C. J. 2006, ApJ, 638, 686
Cowie, L. L., Songaila, A., Hu, E. M., & Cohen, J. G. 1996, AJ, 112, 839
Cox, T. J., Jonsson, P., Primack, J., & Somerville, R. S. 2006, MNRAS, 373, 1013
Cox, T. J., Primack, J., Jonsson, P., & Somerville, R. S. 2004, ApJ, 607, L87
Croton, D. J., et al. 2006, MNRAS, 365, 11
Dekel, A., & Birnboim, Y. 2006, MNRAS, 368, 2
Dekel, A., & Silk, J. 1986, ApJ, 303, 39
Di Matteo, T., Springel, V., & Hernquist, L. 2005, Nature, 433, 604
Elmegreen, D. M., Elmegreen, B. G., Ravindranath, S., & Coe, D. A. 2007, ApJ, 658, 763
Fan, X., et al. 2004, AJ, 128, 515
Ferrarese, L., & Ford, H. 2005, Space Sci. Rev., 116, 523
Franceschini, A., et al. 2005, AJ, 129, 2074
Genzel, R., et al. 2006, Nature, 442, 786
Giallongo, E., Salimbeni, S., Menci, N., Zamorani, G., Fontana, A., Dickinson, M., Cristiani, S., & Pozzetti, L. 2005, ApJ, 622, 116
Guainazzi, M., Piconcelli, E., Jimenez-Bailon, E., & Matt, G. 2005, A&A, 429, L9
Hasinger, G., Miyaji, T., & Schmidt, M. 2005, A&A, 441, 417
Hopkins, P. F., Hernquist, L., Cox, T. J., Di Matteo, T., Robertson, B., & Springel, V. 2006, ApJS, 163, 1
Kauffmann, G., et al. 2003, MNRAS, 346, 1055
Komossa, S., Burwitz, V., Hasinger, G., Predhel, P., Kaastra, J. S., & Ikebe, W. 2003, ApJ, 582, L15
Lacey, C. G., & Cole, S. 1993, MNRAS, 262, 627
Lapi, A., Cavaliere, A., & Menci, N. 2005, ApJ, 619, 60
Lapi, A., Shankar, F., Mao, J., Granato, G. L., Silva, L., De Zotti, G., & Danese, L. 2006, ApJ, 650, 42
McLure, R. J., & Dunlop, J. S. 2004, MNRAS, 352, 1390
Menci, N., Cavaliere, A., Fontana, A., Giallongo, E., & Poli, F. 2002, ApJ, 575, 18
Menci, N., Cavaliere, A., Fontana, A., Giallongo, E., Poli, F., & Vittorini, V. 2003, ApJ, 587, L63
Menci, N., Fontana, A., Giallongo, E., & Salimbeni, S. 2005, ApJ, 632, 49
Mo, H. J., Mao, S., & White, S. D. M. 1998, MNRAS, 295, 319
Panessa, F., Bassani, L., Cappi, M., Dadina, M., Barcons, X., Carrera, F. J., Ho, L. C., & Iwasawa, K. 2006, A&A, 455, 173
Peebles, P. J. E. 1993, Principles of Physical Cosmology (Princeton: Princeton Univ. Press)
Sandage, A. 2005, ARA&A, 43, 581
Somerville, R. S., & Primack, J. R. 1999, MNRAS, 310, 1087
Somerville, R. S., Primack, J. R., & Faber, S. M. 2001, MNRAS, 320, 504
Spergel, D. N., et al. 2007, ApJS, 170, 377
Strateva, I., et al. 2001, AJ, 122, 1861
Vanden Berk, D. E., et al. 2006, AJ, 131, 84
Vestergaard, M. 2004, ApJ, 601, 676
Vittorini, V., Shankar, F., & Cavaliere, A. 2005, MNRAS, 363, 1376